Analyzing the Behavior of Different NACA Profiles at Different Angles of Attack In a Flow Field

Landon Knipp

Abstract

By the beginning of the 20th century, many aerodynamics engineers were becoming familiar with how different geometries behaved differently under the same conditions, such as similar orientations in respect to the direction of their motion, and at certain speeds. Mathematics was used in order to derive solutions for simple geometries, but when it came to more complex shapes that worked better for specific applications, it was left for trial and error. With modern technology, such as advanced computing methods, it is possible to model different geometries to see how they perform generically. This is how many advancements in aerospace technology have been curated in the past couple decades.

1 Introduction

The goal is to determine how different geometries inherently carry different characteristics. The main characteristics that are being evaluated are pressure distributions along an airfoil's surface, coefficients of lift and drag, and separation points in reference to the chord length. All of these attributes are evaluated at different angles of attack. The angle of attack is simply the angle the flow of the fluid makes with the orientation of the airfoil's chord (an imaginary line that connects the leading edge with the trailing edge). The two airfoil profiles analyzed were invented by the National Advisory Committee for Aeronautics (NACA), whom in 1929 began systematizing different geometries of airfoils in order to understand clearly their aerodynamic properties. These two profiles are given the names NACA 0012 and NACA 4412.

The names of each profile were systematized in a way to where all of the information of its geometry is described by the numbers. The first digit describes the maximum camber of the airfoil as the percentage of the chord length. The second digit describes the maximum camber location in tenths of the chord. The third and fourth digits report the maximum section thickness as a percentage of the chord length. Notice how everything is related to the chord, so everything is scaled up the same way for every type of airfoil. With this information, we know that the NACA 0012 profile is symmetric about its top and bottom surfaces because there is no camber, and its thickest portion is 12% of the chord. The NACA 4412 profile has a maximum camber that is 4% of the chord and this is located at 40% of the chord length in reference from the leading edge.

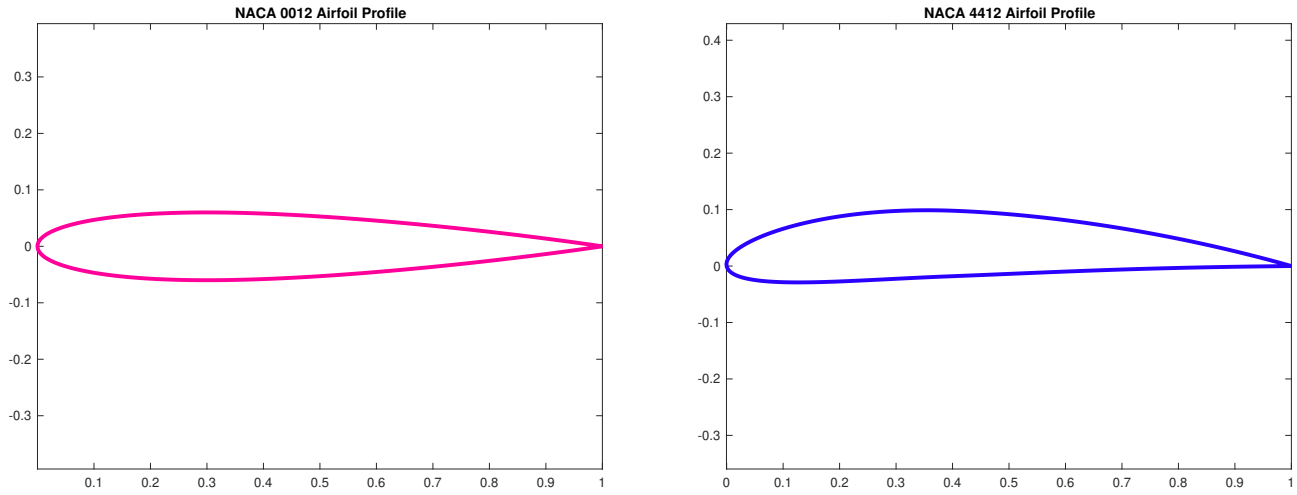

(a) NACA 0012 (b) NACA 4412

Figure 1: Side View of Airfoil Profiles

2 Code Implementation

The main concepts used from Project 2 (vortex panel method) were applied to analyzing the two airfoil profiles. Recall that matrices were formed consisting of several coefficients based on the orientation of each panel. For N number of panels that form a closed looped simulating the geometry, there are N + 1 number of boundary points. This was enforced so that the geometry was closed, and that we were able to apply the Kutta condition (simulating where the flow left the cylinder in the previous project). Here, the Kutta condition is not enforced since the airfoils are not radially symmetrical. We needed to change the placement of the Kutta condition for the cylinder because it is radially symmetric, and its orientation then does not affect the pressure forces acting on it. For the airfoils, what we will be changing is the angle of attack. We still want to have N + 1 boundary points to clarify that the geometry is closed (to incorporate the last panel).

Recall that after determining the velocity at each control point, the normalized coefficient of pressure is:

$$C_P = 1 - V^2 \tag{1}$$

The method of pressure forces was used to determine the total lift force; however, since we want to keep all of our values normalized, the typical equation (using outward normal vectors) for pressure-forces turns into:

$$(C_{F_x}, C_{F_y}) = \sum_{i=1}^{N} C_{P_i}(-\hat{n}_i)S_i \tag{2}$$

C_{F_x} and C_{F_y} are the coefficients of the forces in the x and y directions, respectfully. In order to get from these to the coefficients of lift and drag, the following matrix calculation is performed:

$$\begin{bmatrix} C_D \\ C_L \end{bmatrix} = \begin{bmatrix} cos(\alpha) & sin(\alpha) \\ -sin(\alpha) & cos(\alpha) \end{bmatrix} \begin{bmatrix} C_{F_x} \\ C_{F_y} \end{bmatrix}$$

To determine the points of separation for a variety of angle of attacks, Thwaite's Method is used:

$$K(x_s) = \frac{0.45}{U_e^6(x_s)}(\frac{dU_e}{dx}(x_s)) \int_0^{x_s} U_e^5(\xi)d\xi = -0.09 \tag{3}$$

Note that x_s is the critical distance along the surface that a fluid parcel has travelled when it begins to separate from the body. Thwaite's Method was computed for a variety of angles of attack. Instead of simply using x_s when plotting, the distance on the graph (the horizontal axis) is the distance of the chord. This way, it is simple to see at what angle of attack the airfoil experiences separation on the top surface at 20% the chord length. This is the value used to determine the stall angle for these cases. The stall angle is a critical angle when an airfoil achieves maximum lift. After this angle, giant eddies begin to shed off the back side of the body, dramatically increasing the amount of drag, and create massive moments (torques) on the body.

In order to determine the relevancy of the data gathered from the computations, the analytical solution resulting from thin airfoil theory was referred to. The assumptions of thin airfoil theory are that the thickness of the airfoil can be ignored, and we imagine that the top and bottom surfaces are collapsed onto the mean camber-line. Therefore, the circulation values along the airfoil become:

$$\gamma(\xi) = u_2(\xi) - u_1(\xi) \tag{4}$$

where u_2 is the velocity on the bottom-side and u_1 is the velocity on the top-side. We assume that all angles in reference to each other are small, so $sin(\epsilon) \approx \epsilon$, $cos(\epsilon) \approx 1$, and $arctan(\epsilon) \approx \epsilon$. From these assumptions, we arrive with:

$$U\alpha = \frac{1}{2\pi} \int_0^c \frac{\gamma(\xi)}{x - \xi} d\xi \tag{5}$$

Eventually we come up with the coefficient of lift for a thin airfoil as:

$$C_L = 2\pi\alpha_a \tag{6}$$

$$\alpha_a = \alpha - \alpha_{L_0} \tag{7}$$

where α_a represents the absolute angle of attack: $\alpha_a = \alpha + \alpha_{L_0}$. α_{L_0} is the angle at which an airfoil experiences no lift. This is not necessarily at 0° for all bodies because some geometries create a non-zero lift situation at no angle of attack. For the NACA 0012 profile $\alpha_{L_0} = 0^\circ$, but for the NACA 4412 airfoil $\alpha_{L_0} = -4.15^\circ$. Note how this means that this specific airfoil profile has zero lift tilted down slightly.

3 Results

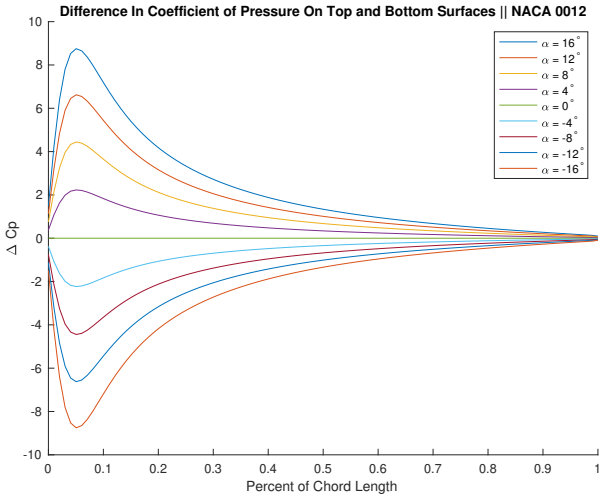

(a) ΔC_P for NACA 0012

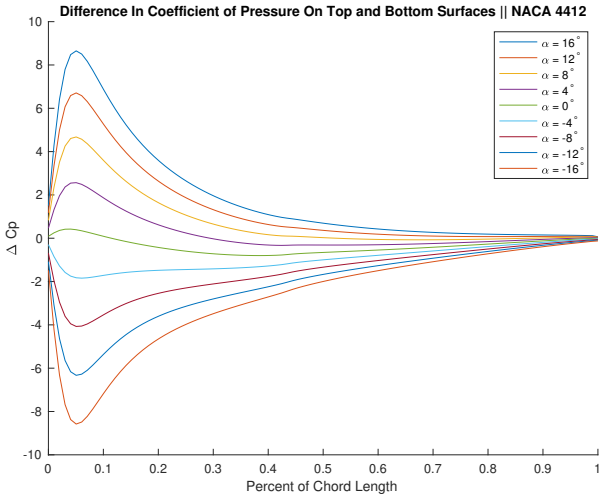

(b) ΔC_P for NACA 4412

Figure 2: Difference In Coefficient of Pressure from Top and Bottom Surfaces

The above figure shows the difference in coefficient of pressure between the top and bottom surfaces of both airfoils. Due to the symmetric nature of the NACA 0012 geometry, there is no difference in pressure for no angle of attack. Furthermore, positive and negative angles of attack are mirrored. This makes sense due to how the fluid experiences the same amount of curvature, and the exact opposite at negative to positive rotations.

However, for the NACA 4412 geometry, the curvature on the bottom-side is not the same as the top. This is noticeable if you look at when $\alpha = 0$ specifically because there is an upward bump at the far left side and then dives below zero for the remainder of the curve. Referring back to α_{L_0}, this data explains why there is some amount of lift even when there is no angle of attack of the NACA 4412 profile.

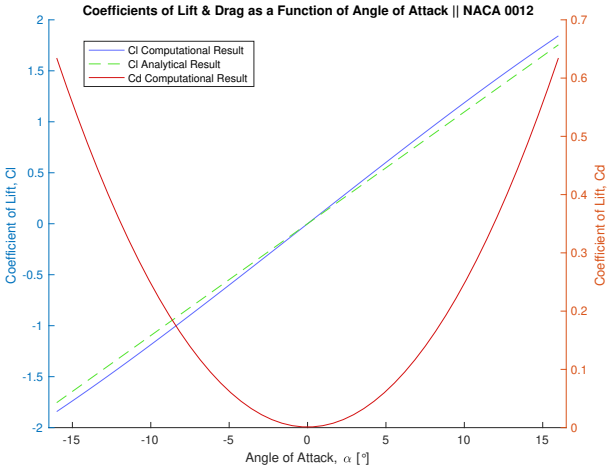

(a) C_L and C_D for NACA 0012

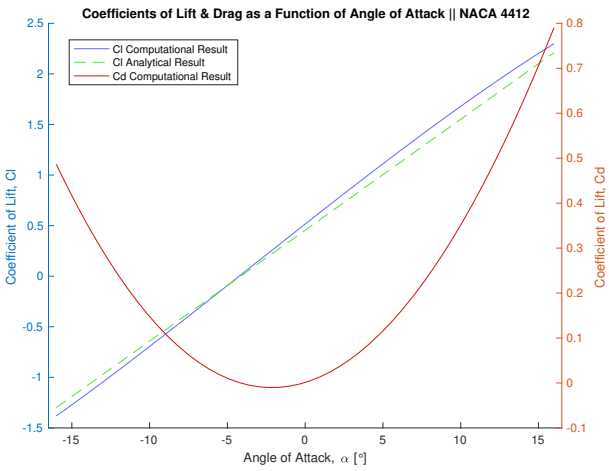

(b) C_L and C_D for NACA 4412

Figure 3: Coefficients of Lift and Drag For Different Angles of Attack

In Figure (3), it is noticeable how there is a greater coefficient of lift for the NACA 4412 profile than for the NACA 0012 geometry. This again relates back to the inherent geometry of the NACA 4412 profile. The curve is shifted to the left because of α_{L_0}. Therefore, it experiences higher coefficients of lift for the same angle of attack in comparison to the NACA 0012 profile.

The coefficient of drag is much smaller than the coefficient of lift because in the calculations, the models were constructed as an idealized flow, where there is no viscosity, no boundary layers forming, and is considered to be incompressible. Due to these parameters, it is expected to not see much drag at all. The drag from the calculations comes from using pressures-forces at each control point, given from the coefficients of pressure in Figure (2). At high magnitudes of α, the drag increases because there is more surface area normal to the direction of the flow (and pressure forces always act normal to a surface).

To scale from the coefficients to the actual values of lift and drag, all we have to do is multiply them by the dynamic pressure: $q_\infty = \frac{1}{2}\rho U_\infty^2$. However, this results in lift per span, L', and drag per span, D', (since we do not account for any distance of the wing into nor out of the page).

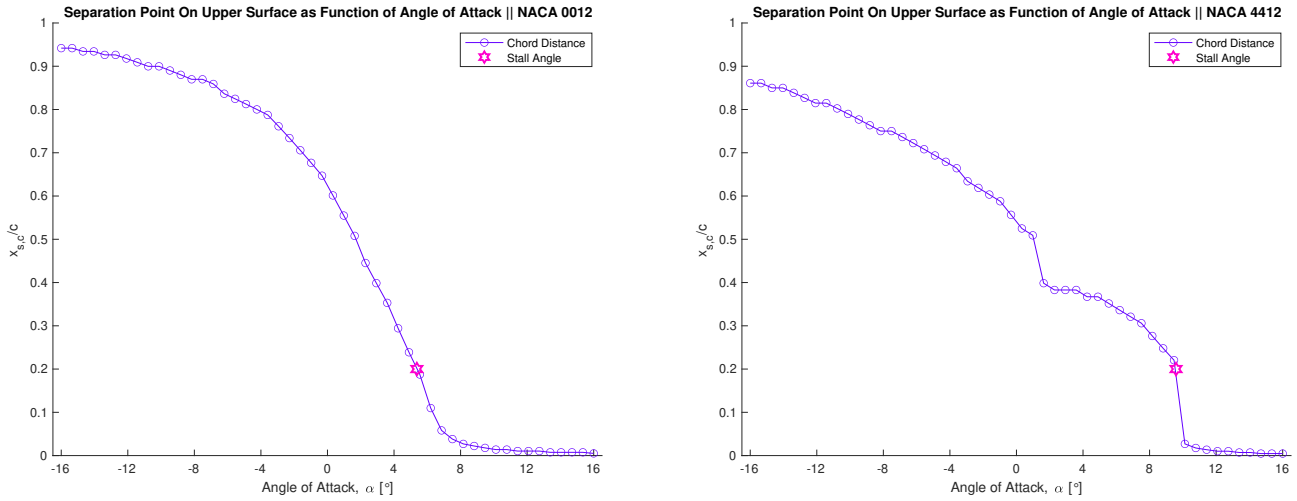

(a) Separation symmetric

(b) Separation cambered

Figure 4: Separation Points on Top Surface For Different Angles of Attack

Airfoil Profile	Computational Result	Experimental Result	Reynold's Number
NACA 0012	5.3720°	12°	6×10^9
NACA 4412	9.5902°	14°	6×10^9

The experimental results for the stall angles were taken from *Theory of Wing Sections, Appendix IV*, by Albert Edward Von Doenhoff and Ira Abbott. The values chosen for the Reynold's Number is 6×10^9 over the other value they had data collected from ($Re = 9 \times 10^9$) because we assumed to have an idealized flow. The Reynold's Number in the table above is more laminar than the other one, so it is more fitting to the vortex panel method. The values are quite different, specifically for the NACA 0012 profile.

There are several reasons why they are not equivalent. First, in a real life scenario, flow is compressible. Boundary layers form, creating small vortices along the surface of the body. These boundary layers also cause a shearing stress on the airfoil. The texture of the surface also plays a huge roll in the stall angle because a rougher surface will cause the flow to trip up sooner than for a smooth surface, changing the location where the flow separates. The surface for the experimental results was labelled as having a

'standard roughness'. Other properties such as temperature and heat transfer are also important. All of the values were normalized in the calculations in order to get a broad idea of how each airfoil would perform under different angles of attack for a generic flow. There was no specific speed assumed, no particular far field pressure, and no input for the density of the fluid medium. The computational results give a completely general solution for the stall angles, and these values would change if we specified the situation (i.e. what fluid the airfoils are travelling in). If we wanted to see how accurate our data truly is in comparison to the experimental results found in the literature, we would have to scale our normalized results based on the conditions in the experiments, which are given by the Reynold's Number. For an airfoil, the Reynold's Number is typically described as: $Re_c = \frac{\rho U_\infty c}{\mu}$. ρ is the density of the fluid, U_∞ is the speed at which the airfoil travels (also known as the far field velocity based on reference frame), c is the length of the chord, which we normalized to a distance of one unit, and μ is known as the dynamic viscosity of the fluid.

4 Discussion

The coefficients of lift as seen in Figure (6) are similar to the coefficients of lift found experimentally for the NACA 0012 and NACA 4412 profiles in literature by Von Doenhoff and Abbott. The main difference is where the values begin to deviate more as the magnitude of the angle of attack approaches 16°. This is due to viscous effects of a real fluid, which are not taken into consideration with the vortex panel method. Therefore, for when $-10° \leq \alpha \leq 10°$, the data from the computations is extremely close to the experimental values. I referred to the coefficients of lift for the case when $Re = 6 \times 10^9$ with what the literature refers to as 'standard roughness'. In order to build models that reflect the real world more accurately, methods deviating away from ideal flow solutions. Incorporating effects from the boundary layers and shearing forces that perturb the flow along the surface will give more accurate solutions. However, for as simple as the vortex panel method is, it does a surprisingly accurate job at modelling coefficients of lift for the NACA 0012 and NACA 4412 profiles.

References

[1] Abbott, Ira and Edward Von Doenhoff, Albert. *Theory of Wing Sections*. Dover Publications, Inc. 1959

[2] Knipp, Landon. *Project 2*. 2021

[3] Kuethe, A. M. and Chow, C-Y. *Foundations of aerodynamics*. 5th edition. Wiley 1998.